

## CRITICAL STATE BEHAVIOR OF A COMPACTED SILT SPECIMEN

TRINH MINH THU<sup>i)</sup>, HARIANTO RAHARDJO<sup>ii)</sup> and ENG-CHOON LEONG<sup>iii)</sup>

### ABSTRACT

Shear strength of unsaturated soil is commonly obtained from a consolidated drained (CD) triaxial test. However in many field situations, fill materials are compacted where the excess pore-air pressure developed during compaction will dissipate instantaneously, but the excess pore-water pressure will dissipate with time. This condition can be simulated in a constant water content (CW) triaxial test. The critical states of an unsaturated soil obtained from the CW and the CD triaxial tests have not been extensively investigated and compared. A series of CW and CD triaxial tests was carried out on a statically compacted silt. The results from this study show that the critical state lines at different matric suctions on the ( $q$ - $p$ ) plane were parallel with a slope of 1.28 for both the CW and CD triaxial tests, indicating the unique relationship between deviator stress and mean net stress. The results also indicate the unique relationship between the specific volume,  $v$ , and mean net stress,  $p$ , on the ( $v$ - $p$ ) plane for both the CW and CD triaxial tests. The slope of the critical state lines on the ( $v$ - $p$ ) plane for both the CW and CD triaxial tests decreased with the increase in matric suction.

**Key words:** consolidated drained triaxial tests, constant water content triaxial tests, critical state, matric suction, unsaturated soil (IGC: D5/D6)

### INTRODUCTION

In many field situations, fill materials are compacted where the excess pore-air pressure developed during compaction will dissipate instantaneously, but the excess pore-water pressure will dissipate with time. It can be considered that the air phase is generally under a drained condition and the water phase is under an undrained condition during loading. This condition can be simulated in a constant water content (CW) triaxial test. The excess pore-water pressure generated during loading under the constant water content condition is an important aspect that may cause many geotechnical problems such as slope failures. However, shear strength parameters used in geotechnical designs are obtained mainly from the consolidated drained (CD) or consolidated undrained (CU) triaxial tests. In the past few decades, numerous researchers (Bishop et al., 1960; Bishop and Donald, 1961; Blight, 1961; Satija, 1978; Sivakumar, 1993; Rahardjo et al., 2004) have studied the shear strength characteristics of unsaturated soils under the constant water content condition in a triaxial apparatus. The difficulty of the CW test is associated with the assurance for uniformity of the pore-water pressure within the soil specimen during shearing.

A number of researchers (Alonso et al., 1990; Toll, 1990; Sivakumar, 1993; Maatouk et al., 1995; Wheeler,

1996; Cui and Delage, 1996; Bolzon et al., 1996; Adam and Wulfsohn, 1998; Rampino et al., 2000; Sun and Mat-suoka, 2000; Tang and Graham, 2002; Chiu and Ng, 2003) have studied the critical state of unsaturated soil on the ( $q$ - $p$ ) plane (where  $q$  = deviator stress =  $(\sigma_1 - \sigma_3)$  and  $p$  = mean net stress =  $[(\sigma_1 + \sigma_2 + \sigma_3)/3 - u_a]$ ). However, the experimental data of unsaturated soil on the ( $q$ - $s$ - $p$ ) space and ( $v$ - $p$ ) plane have not been extensively investigated (where,  $s$  = matric suction and  $v$  = specific volume). The main objective of this paper is to study the soil parameters at the critical state as obtained from the CW and CD triaxial tests. In addition, the soil parameters at the critical state obtained from the CW and the CD triaxial tests are compared.

Identically compacted kaolin specimens at the maximum dry density ( $1.35 \text{ Mg/m}^3$ ) and optimum water content (22%) were prepared for triaxial testing. Specimens were statically compacted in 10 layers of equal thickness of 10 mm. The height and diameter of the final specimens were 100 mm and 50 mm, respectively. The concept of axis translation technique (Hilf, 1956) was adopted to control matric suction in the soil specimens during both tests.

### SOIL PROPERTIES

Coarse kaolin made by Kaolin Malaysia SDN BHD

<sup>i)</sup> Head, Department for Academic affairs and Head, Division of Geotechnical Engineering, Hanoi Water Resources University, Vietnam.

<sup>ii)</sup> Professor, School of Civil and Environmental Engineering, Nanyang Technological University, Singapore (chrahardjo@ntu.edu.sg).

<sup>iii)</sup> Associate Professor, ditto.

The manuscript for this paper was received for review on August 7, 2006; approved on March 26, 2007.

Written discussions on this paper should be submitted before March 1, 2008 to the Japanese Geotechnical Society, 4-38-2, Sengoku, Bunkyo-ku, Tokyo 112-0011, Japan. Upon request the closing date may be extended one month.

**Table 1. Index properties of the statically compacted silt specimen**

Soil properties	Value
Specific gravity, $G_s$	2.65
Liquid limit, LL (%)	51.0
Plastic limit, PL (%)	36.5
Plasticity index, PI (%)	15.4
Clay (%)	15.0
Silt (%)	85.0
Unified Soil Classification System (USCS)	MH (silt of high plasticity)
Maximum dry unit weight, $\rho_{d \max}$ (Mg/m <sup>3</sup> )	1.35
Optimum water content, $w_{opt}$ (%)	22.0
Coefficient of permeability at saturated, $k_s$ (m/s)	$6.4 \times 10^{-8}$

was selected for the experimental program in this study. The Atterberg Limits, grain size analysis, specific gravity and coefficient of permeability tests were conducted to determine the index properties of the compacted kaolin. The index properties of the kaolin are presented in Table 1.

## PROCEDURE AND TESTING PROGRAM

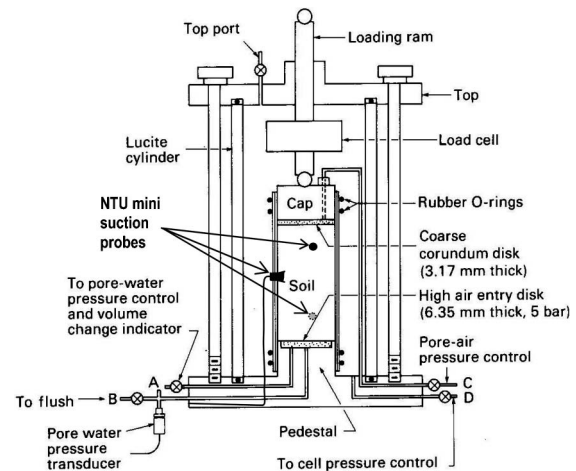
The modified triaxial apparatus used in this study for the CW and CD triaxial tests was similar to the modified triaxial apparatus described by Fredlund and Rahardjo (1993). The modified triaxial apparatus allows the control of both pore-air,  $u_a$ , and pore-water pressures,  $u_w$ , using the axis-translation technique and therefore, the matric suction,  $(u_a - u_w)$  of the specimen can be controlled. Figure 1 shows the test set up. The height and diameter of the specimens were approximately 100 mm and 50 mm, respectively. Identically compacted silt specimens at the maximum dry density and optimum water content were prepared. The specimens were statically compacted in 10 layers of 10 mm thickness.

### Testing Procedure for Constant Water Content Tests

The testing procedure for the triaxial tests on saturated soils as given by Head (1986) was adopted. The procedure for triaxial tests on unsaturated soils follows the procedure described in Fredlund and Rahardjo (1993). The initial matric suctions of the specimens were established using the axis-translation technique.

### Saturation Stage

The soil specimen was initially saturated for all the tests in order to obtain consistent initial water content and degree of saturation. In this stage, the air pressure line was replaced by water pressure line connected to a digital pressure and volume controller (DPVC) to inject water into the specimen from the top. During the saturation stage, the specimen was saturated by applying a cell pressure,  $\sigma_3$ , and a back pressure,  $u_w$ , under an effective confining pressure of 10 kPa until the pore-water pressure parameter, B, was close to 1. Full saturation was assumed to have been achieved when the B value was greater than 0.95 (Head, 1986). Each specimen required about four

**Fig. 1. Modified triaxial cell for unsaturated soil testing (modified from Fredlund and Rahardjo, 1993)**

days for the saturation stage to be completed.

### Consolidation Stage

After saturation, the soil specimen was isotropically consolidated to the desired net confining stress,  $(\sigma_3 - u_w)$ . During the consolidation stage, the specimen was allowed to consolidate under an isotropic confining stress,  $\sigma_3$ , and a pore-water pressure,  $u_w$ . The magnitudes of the pressures for the consolidation stage were selected based on the desired values of the net confining stress,  $(\sigma_3 - u_a)$ . During the isotropic consolidation, the water valve was left opened and the pressures were controlled at the desired values. The amount of water that drained out from the soil specimen during the isotropic consolidation was recorded by the DPVC and the data were transferred to the personal computer. The total volume change of the specimen during the test was calculated from the volume change on the DPVC which indicated the amount of water that flowed into or out of the triaxial cell. The consolidation was assumed to have been completed when the water volume change leveled off and the excess pore-water pressure had fully dissipated. Each specimen required about 1 hour for the consolidation stage to complete. After the isotropic consolidation had been completed, matric suction was applied to the soil specimen.

### Matric Suction Equalization Stage

Once the consolidation stage had been completed, the line connected to the top loading cap was disconnected from the DPVC and reconnected to the air pressure system. The DPVC was subsequently connected to the pore-water pressure at the base plate (i.e.,  $u_w$ ). During the drying stage, matric suction was increased by decreasing the pore-water pressure at the base plate while maintaining the pore-air pressure. Meanwhile for the wetting stage, matric suction was decreased by increasing the pore-water pressure at the base plate. The amount of water that drained out from the soil specimen and the total volume change of the specimen during drying and wetting stages were recorded by the DPVCs (i.e., DPVC for cell pressure and DPVC for back pressure) and stored

in a personal computer. The equalization was assumed to have been achieved when the excess pore-water pressure had fully dissipated and water volume change had decreased to 0.04% per day as suggested by Sivakumar (1993). All of recorded data were transferred to a personal computer.

#### Shearing Stage

When an equilibrium condition had been achieved under the applied net confining stress,  $(\sigma_3 - u_a)$ , and matric suction,  $s = (u_a - u_w)$ , the specimen was then sheared by applying an axial load at a constant strain rate. Ong (1999) conducted a pilot CW triaxial test to investigate the effect of strain rate on matric suction and shear strength of compacted specimens of the residual soil from the sedimentary Jurong Formation of Singapore. The pilot test was conducted under a constant water content condition with different strain rates ranging from 0.009 to 0.081 mm/min. The peak stresses of all the obtained stress-strain curves were found to coincide. The matric suction at failure increased about 2% when strain rate increased from 0.009 mm/min to 0.018 mm/min. However, the matric suction at failure increased about 10% when strain rate increased from 0.018 mm/min to 0.081 mm/min. Rahardjo et al. (2004) used the strain rate of 0.009 mm/min for the compacted residual soil from the sedimentary Jurong Formation. In this study, the strain rate of 0.009 mm/min was also used because the silt had similar properties (i.e., plasticity index, coefficient of permeability) with the properties of the residual soil from the sedimentary Jurong Formation of Singapore. The soil specimen was sheared under drained conditions for the air phase and undrained conditions for the water phase. This means that during shearing the valve for the air pressure line was opened and controlled at a required pressure while the valve for the water pressure line was closed. In this shearing stage, the pore-air pressure,  $u_a$ , was maintained at the same magnitude as that obtained at the end of the equalization stage. The pore-water pressure,  $u_w$ , in the soil specimen would increase or decrease depending on the volume change of the soil specimen and this pore-water pressure was measured using NTU mini suction probes. The difference between the pore-air pressure,  $u_a$ , and the pore-water pressure,  $u_w$ , gives the matric suction,  $(u_a - u_w)$ . Shearing was terminated when the deviator stress,  $q = (\sigma_1 - \sigma_3)$ , reached a constant value or a distinct shear plane in the specimen had been observed. The maximum axial strain was set to 20%. Each specimen required about one to three days for the shearing stage to be completed.

#### Testing Procedure for the CD Triaxial Tests

Saturation, Consolidation and Matric Suction Equalization Stages

The saturation, consolidation and matric suction equalization stages were conducted in the same manner as those performed in the CW triaxial tests. Once the matric suction equalization had been completed, the specimen was sheared under a drained condition.

#### Shearing Stage

Rahardjo et al. (2004) used the strain rate of 0.0009 mm/min for the CD triaxial tests on the compacted residual soil from the sedimentary Jurong Formation. In this study, the strain rate of 0.0009 mm/min was also used because the silt had similar properties (i.e., plasticity index, coefficient of permeability) with the properties of the residual soil from the sedimentary Jurong Formation. The soil specimen was sheared under drained conditions for both the air and water phases. This means that during shearing the valves for both the air pressure and water pressure lines were opened and controlled at the required pressures. In this shearing stage, the pore-air pressure,  $u_a$ , and pore-water pressure,  $u_w$ , were maintained at the same magnitudes as those obtained at the end of the equalization stage. Shearing was terminated when the deviator stress,  $q = (\sigma_1 - \sigma_3)$ , reached a constant value or a distinct shear plane in the specimen had been observed. The maximum axial strain was set to 20%.

### TEST RESULTS AND DISCUSSIONS

A naming convention for the CW tests was adopted using a designation of CW $x$ - $y$ . The term  $x$ - $y$  in CW $x$ - $y$  means that the test was conducted under a net confining pressure of  $x$  kPa and at an initial matric suction of  $y$  kPa. Similarly, a naming convention for the CD tests also used a designation of CD $x$ - $y$ . The term  $x$ - $y$  in CD $x$ - $y$  means that the test was conducted under a net confining pressure of  $x$  kPa and a matric suction of  $y$  kPa.

Figure 2 shows the results from the CW triaxial shearing tests under different net confining stresses but at the same initial matric suction of 150 kPa. The graphs in Fig. 2 indicate that most of the stress-strain curves showed evidence of post-peak strain softening.

The results from the CD triaxial shearing tests under different net confining stresses but at the same matric suction of 100 kPa are presented in Fig. 3. Figure 3 shows that most of the stress-strain curves exhibited evidence of post-peak strain softening. However, the ductility of the specimens increased with the increase in the net confining stress. The lower the net confining stress was, the more distinct the peak deviator stress would be. The higher the net confining stress was, the higher the axial strain required for the specimen to reach the maximum deviator

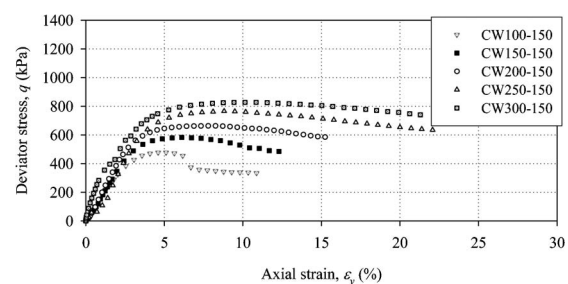


Fig. 2. Deviator stress versus axial strain from the CW triaxial tests under different net confining stresses but at the same initial matric suction of 150 kPa

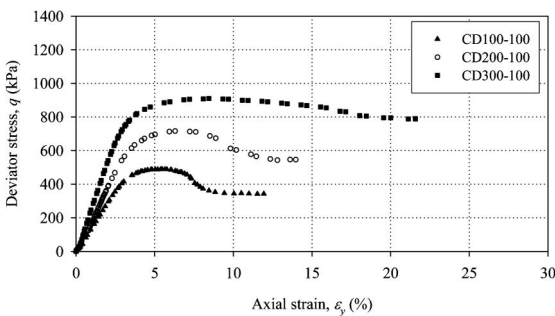


Fig. 3. Deviator stress versus axial strain from the CD triaxial tests under different net confining stresses but at the same matric suction of 100 kPa

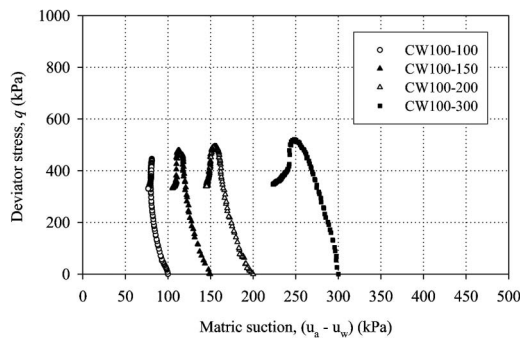


Fig. 4. Stress paths on the  $(q-s)$  plane for the CW triaxial tests under different initial matric suctions but at the same net confining stress of 100 kPa

stress.

Figure 4 shows the stress paths for the CW triaxial tests under different initial matric suctions (i.e., matric suctions of 100 kPa, 150 kPa, 200 kPa and 300 kPa) but at the same net confining stresses of 100 kPa. The results indicate that matric suction decreased with the increase in deviator stress. It can be seen that matric suction decreased throughout the CW triaxial shearing tests. In general, the trend of the stress paths on the  $(q-s)$  plane during the shearing stage was similar. The deviator stresses dropped after reaching the peak deviator stress towards the direction of decreasing matric suctions (i.e., to the left of the graph).

Figure 5 summarizes the critical states of the CW triaxial tests under different net confining stresses and different initial matric suctions (i.e., zero kPa, 100 Pa, 150 kPa, 200 kPa and 300 kPa) on the  $(q-p)$  plane. Figure 5 indicates that the critical state lines at different matric suctions were parallel on the  $(q-p)$  plane. The slopes of the critical state lines for the CW triaxial tests have the same value of 1.28. Figure 6 shows the summary of the critical states of the CW triaxial tests under different net confining stresses and different initial matric suctions on the  $(q-s-p)$  space. The stress states at the critical state of the CW triaxial tests are presented in Table 2.

Figure 7 shows the summary of the critical states of the CD triaxial tests under different net confining stresses and different matric suctions (i.e., 0 kPa, 100 kPa, 200 kPa and 300 kPa) on the  $(q-p)$  plane. Meanwhile, Figure 8

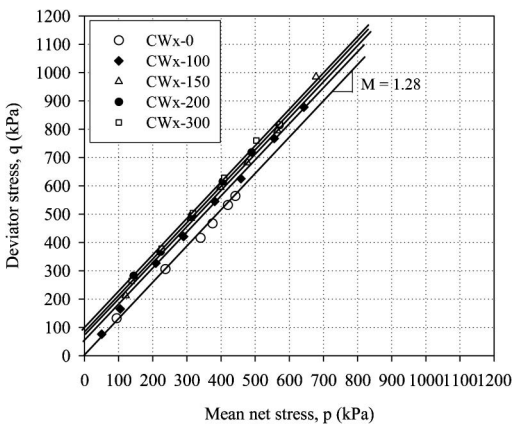


Fig. 5. Critical state lines in the  $(q-p)$  plane from the CW triaxial tests

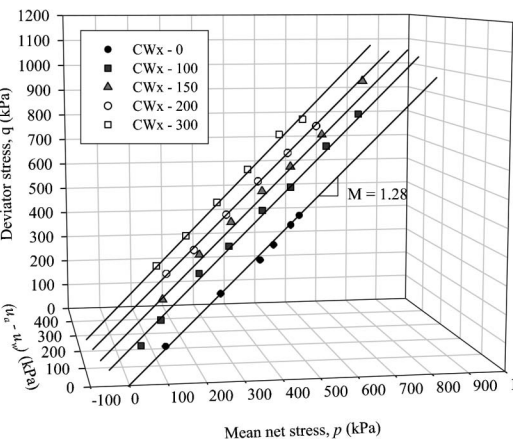


Fig. 6. Critical state lines in the  $(q-s-p)$  space from the CW triaxial tests

Table 2. Stresses at the critical state of the CW triaxial tests

Net confining stress (kPa)	Initial matric suction (kPa)									
	0		100		150		200		300	
	$p$	$q$	$p$	$q$	$p$	$q$	$p$	$q$	$p$	$q$
50	94	132	105	165	121	212	144	282	138	264
100	178	235	209	327	224	371	222	367	226	378
150	267	351	290	421	312	486	315	495	318	504
200	352	457	382	545	398	595	405	615	409	628
250	413	532	458	625	477	682	489	718	503	760
300	437	564	556	767	565	795	571	814	572	817

shows the summary of the critical states of the CD triaxial tests on the  $(q-s-p)$  space. Table 3 presents the stress states at the critical state of the CD triaxial tests.

Figures 5 and 7 indicate that the critical state lines at different matric suctions were parallel on the  $(q-p)$  plane. The slopes of the critical state lines for the CD triaxial tests have the same value of 1.28. In other words, the slopes of the critical state lines on the  $(q-p)$  plane were unique for the compacted silt as obtained from both the CW and CD triaxial tests.

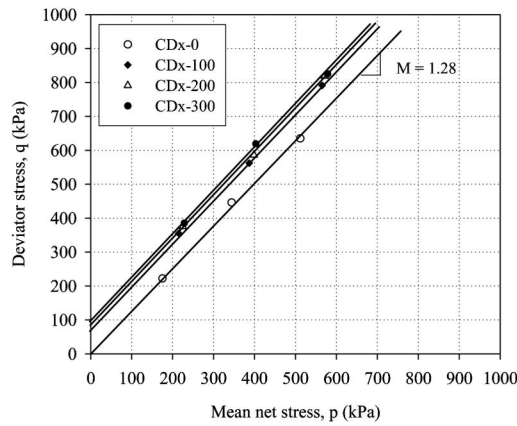


Fig. 7. Critical state lines in the  $(q-p)$  plane from the CD triaxial tests

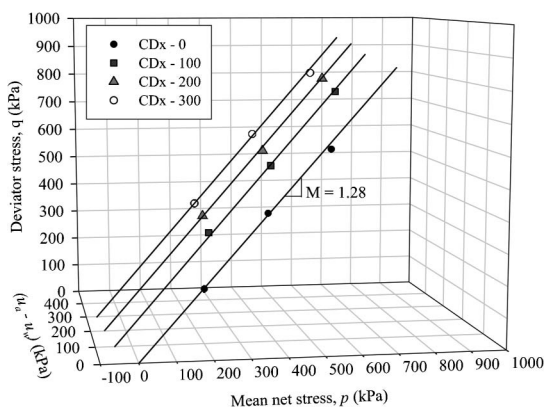


Fig. 8. Critical state lines in the  $(q-s-p)$  space from the CD triaxial tests

Table 3. Stresses at the critical state of the CD triaxial tests

Net confining stress (kPa)	Matric suction (kPa)							
	0		100		200		300	
	$p$	$q$	$p$	$q$	$p$	$q$	$p$	$q$
100	175	225	215	345	225	375	228	385
200	344	432	387	562	399	596	403	609
300	512	635	565	796	572	815	578	835

Figure 9 shows the tensile strength due to matric suction from the CW and CD triaxial tests on the compacted silt specimens under different net confining stresses and at different matric suctions. Figure 9 indicates the non-linear relationship between the tensile strength and matric suction as obtained from the CW and CD triaxial tests in this study agreed with the trend reported by Rampino et al. (1999).

Figure 10 shows the stress paths on the specific volume,  $v$ , (i.e.,  $v = 1 + e$ , where:  $e$  = void ratio) versus logarithm of the mean net stress,  $p$ , for the CD triaxial tests under the saturated condition. Figure 10 shows that the three compacted silt specimens started the shearing process along the normal compression line. The specific volume decreased and then increased subsequently for specimens

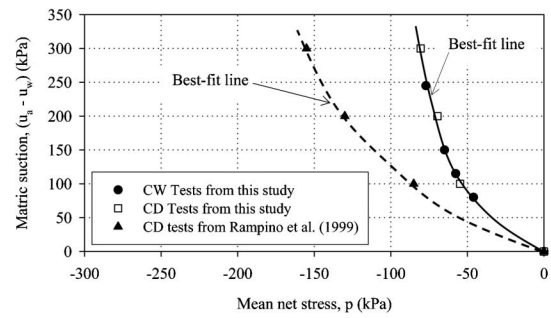


Fig. 9. The tensile strength due to matric suction from CD triaxial tests for the compacted silt specimens

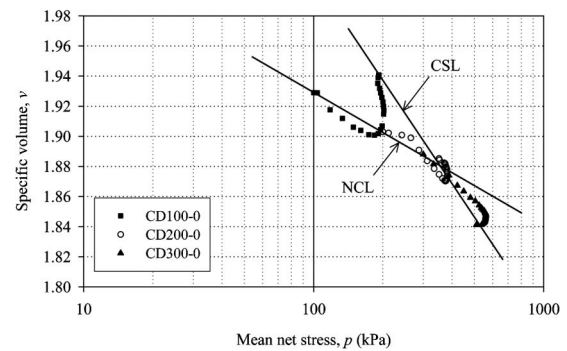


Fig. 10. Stress paths on the  $(v-p)$  plane from the CD tests under saturated condition

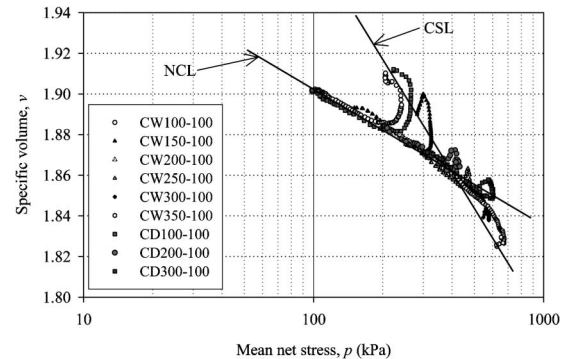


Fig. 11. Stress paths on the  $(v-p)$  plane from the CW and CD tests under matric suction of 100 kPa

CD100-0 and CD200-0. However, the specific volume of specimen CD300-0 decreased throughout the entire shearing stage. Nevertheless, the specific volumes of the saturated CD triaxial tests at the critical state fall on a single straight line, giving the critical state line on the  $(v-\ln p)$  plane. Figure 10 indicates that the slope of the critical state line at saturation on the  $(v-p)$  plane (i.e.,  $\omega(0)$ ) was greater than the slope of the normal compression line (i.e.,  $\lambda(0)$ ). Figures 11 to 14 show the stress paths for the CW and CD triaxial tests under different net confining stresses but at the same matric suctions of 100 kPa, 150 kPa, 200 kPa, and 300 kPa. It appears that the stress paths for the CW and CD triaxial tests showed similar trends. The specific volume decreased at the early stage of

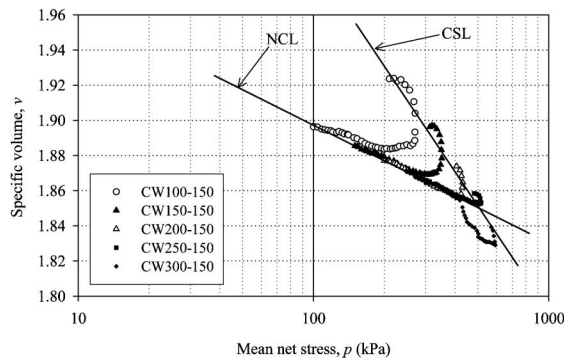


Fig. 12. Stress paths on the  $(v-p)$  plane from the CW tests under matrix suction of 150 kPa

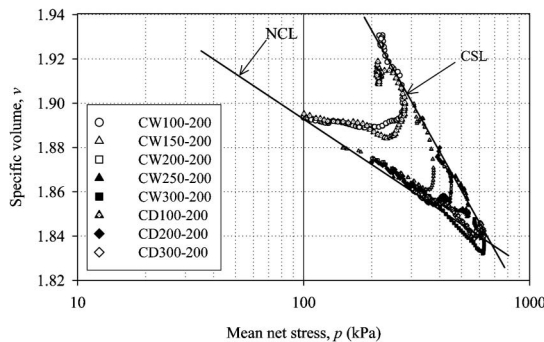


Fig. 13. Stress paths on the  $(v-p)$  plane from the CW and CD tests under matrix suction of 200 kPa

shearing and then increased afterwards. The higher the net confining stress was, the higher the increase in specific volume would be during shearing. However, specimens CW300-100, CW300-150, CW300-200, CW300-300, CD300-0, CD300-100 and CD300-200 underwent compression throughout the entire shearing stage. It can be seen that, the higher the net confining stress was, the higher the compression would be. This could be due to the fact that, the high net confining stress in the soil specimen caused a decrease in the overconsolidation of the soil specimen. As a result, the soil specimen would be compressed during entire shearing stage.

Figures 15 and 16 show the summary of the specific volume versus logarithm of the mean net stress at the critical state for the CW and CD triaxial tests, respectively. There appears to be a linear relationship between the specific volumes with respect to logarithm of mean net stress under a constant matrix suction plane. Figures 15 and 16 indicate that the slope of the critical state line,  $\omega(s)$ , decreased with the increase in matrix suction. In other words, a higher matrix suction resulted in an increase in stiffness of the soil specimen. As a result, the slope of the critical state line decreased with the increase in matrix suction. Figure 17 shows the slope of the critical state line,  $\omega(s)$ , versus matrix suction for the CW and CD triaxial tests. The results from the CW and CD triaxial tests indicate that there is a unique relationship between the slopes of the critical state lines with respect to matrix

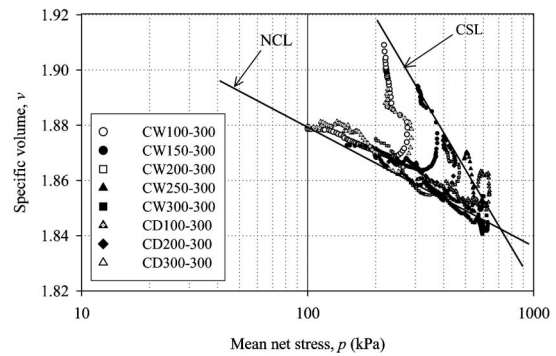


Fig. 14. Stress paths on the  $(v-p)$  plane from the CW and CD tests under matrix suction of 300 kPa

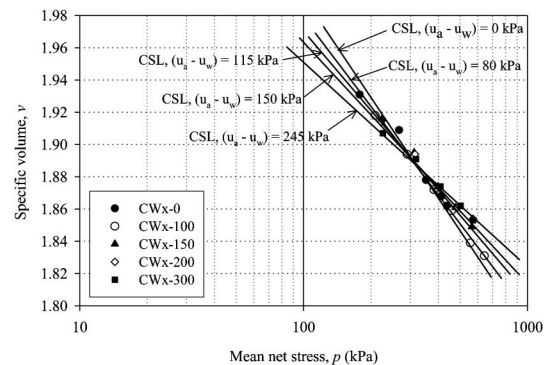


Fig. 15. Critical state lines on the  $(v-p)$  plane from the CW triaxial tests under different matrix suctions

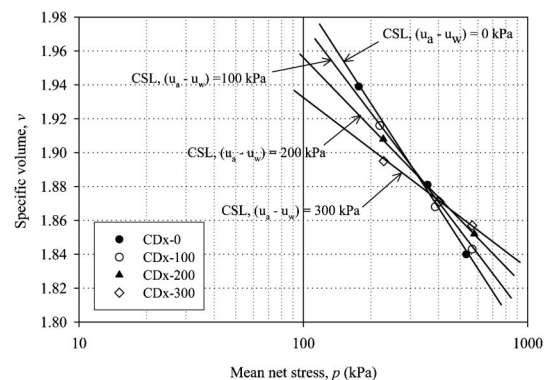


Fig. 16. Critical state lines on the  $(v-p)$  plane from the CD triaxial tests under different matrix suctions

suction. The slopes of the critical state lines,  $\omega(s)$ , on the  $(v-p)$  plane for the CW and CD triaxial tests at the saturated condition and at the matrix suction of 300 kPa were found to be 0.113 and 0.041, respectively. The results from the CW and CD triaxial tests show that the specific volume appeared to remain at the same value under the same matrix suction value. Figure 18 plots the specific volume at the reference stress of 100 kPa (i.e.,  $I(s)$ ) of the critical state lines versus matrix suction. The specific volume at the reference stress also decreased with the increase in matrix suction for the CW and CD triaxial tests.

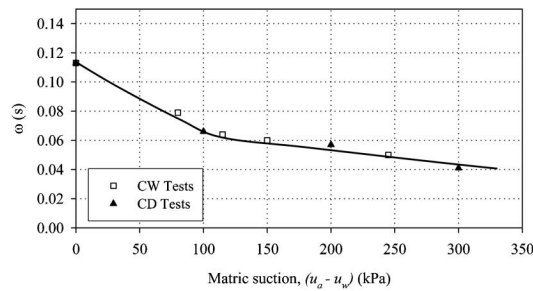


Fig. 17. Slopes of the critical state line versus matric suction

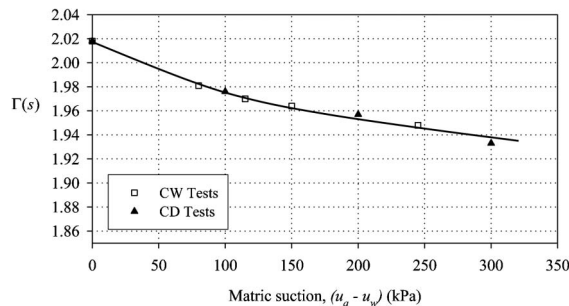


Fig. 18. Specific volume at the reference stress versus matric suction

The unique relationship between the specific volume at the reference stress with respect to matric suction can be obtained from the CW and CD triaxial tests from this study.

## CONCLUSIONS

The critical state lines at different matric suctions on the ( $q$ - $p$ ) plane were parallel with a slope of 1.28 for both the CW and CD triaxial tests. This indicated the unique relationship between the deviator stress and mean net stress for both the CW and CD triaxial tests. The linear relationship between the specific volume and mean net stress for both the CW and CD triaxial tests was obtained from this study. The slope of the critical state on the ( $v$ - $p$ ) plane is similar for both the CW and CD triaxial tests under the same matric suction. The specific volume at reference stress also showed similar values for both CW and CD triaxial tests under the same matric suction. The results also indicated the unique relationship between the specific volume and mean net stress on the ( $v$ - $p$ ) plane for both the CW and CD triaxial tests. The slope of the critical state line on the ( $v$ - $p$ ) plane of both the CW and CD triaxial tests decreased with the increase in matric suction. The unique relationship between the specific volume and mean net stress for both the CW and CD triaxial tests was also observed in this study.

## ACKNOWLEDGMENT

The research is supported by a research grant No. RG 7/99 from the Nanyang Technological University, Singapore. The first author acknowledges the research scholar-

ship received from NTU, Singapore.

## REFERENCES

- Adam, B. A. and Wulfsohn, D. (1998): Critical-state behavior of an agricultural soil, *Journal of Agricultural Engineering Research*, **70**, 345–354.
- Alonso, E. E., Gens, A. and Josa, A. (1990): A constitutive model for partially saturated soils, *Geotechnique*, **40**, 405–430.
- ASTM (2003): *D698–91, Standard Test Methods for Laboratory Compaction Characteristics of Soil Using Standard Effort* (12,400 ft-lb/ft (600 kN-m/m<sup>3</sup>)).
- Bishop, A. W., Alpan, I., Blight, G. E. and Donald, I. B. (1960): Factors controlling the shear strength of partly saturated cohesive soils, *ASCE Research Conference on Shear Strength of Cohesive Soils*, University of Colorado, Colorado, 503–532.
- Bishop, A. W. and Donald, I. B. (1961): The experimental study of partly saturated soil in the triaxial apparatus, *Proc. 5th ICSMFE*, Paris, **1**, 13–21.
- Blight, G. E. (1961): Strength and consolidation characteristics of compacted soil, *PhD. Dissertation*, University of London, London, UK.
- Bolzon, G. Schrefler, B. A. and Zienkiewicz, O. C. (1996): Elastoplastic soil constitutive laws generalized to partially saturated states, *Geotechnique*, **46**, 279–289.
- Chiu, C. F. and Ng, C. W. W. (2003): A State-dependent elastoplastic model for saturated and unsaturated soils, *Geotechnique*, **53**(9), 809–829.
- Cui, Y. J. and Delage, P. (1996): Yielding and plastic behaviour of unsaturated compacted silt, *Geotechnique*, **46**(2), 291–311.
- Fredlund, D. G. and Rahardjo, H. (1993): *Soil Mechanics for Unsaturated Soils*, John Wiley and Sons Inc., New York.
- Head, K. H. (1986): *Manual of Soil Laboratory Testing*, John Wiley and Sons, Inc., **3**, 942–945.
- Hilf, J. W. (1956): An investigation of pore-water pressure in compacted cohesive soils, *Ph.D. Dissertation*, Tech. Memo. No. 654, U.S. Dep. of the Interior, Bureau of Reclamation, Design and Construction Div., Denver, C.O.
- Maatouk, A., Leroueil, S. and Rochelle, P. LA. (1995): Yielding and critical state of a collapsible unsaturated silty soil, *Geotechnique*, **45**, 465–477.
- Ong, B. H. (1999): Shear strength and volume change of unsaturated residual soil, *Master of Engineering Thesis*, Nanyang Technological University, Singapore.
- Rahardjo, H., Ong, B. H. and Leong, E. C. (2004): Shear strength of a compacted residual soil from consolidated drained and the constant water content triaxial tests, *Canadian Geotechnical Journal*, **41**, 1–16.
- Rampino, C., Macuso, C. and Vinale, F. (1999): Mechanical behavior of an unsaturated dynamically compacted silty sand, *Italian Geotechnical Journal*, **33**(02), 26–39.
- Rampino, C., Macuso, C. and Vinale, F. (2000): Experimental behavior and modeling of an unsaturated compacted soil, *Canadian Geotechnical Journal*, **37**, 748–763.
- Satija, B. S. (1978): Shear behaviour of partly saturated soils, *Ph.D. Dissertation*, India Institute of Technology, Delhi, India.
- Sivakumar, V. (1993): A critical state framework for unsaturated soil, *Ph.D. Thesis*, University of Sheffield, Sheffield, U.K.
- Sun, D. A. and Matsuoka, H. (2000): Three-dimensional elastoplastic model for unsaturated soils, *Proc. the Asian Conference on Unsaturated Soils* (eds. by Rahardjo, H., Toll, D. G. and Leong E. C.), 153–158.
- Tang, G. X. and Graham, J. (2002): A possible elasto-plastic framework for unsaturated soils with high-plasticity, *Canadian Geotechnical Journal*, **39**, 894–907.
- Toll, D. G. (1990): A framework for unsaturated soils behaviour, *Geotechnique*, **40**, 31–44.
- Wheeler, S. J. (1996): Inclusion of specific water volume within an elasto-plastic model for unsaturated soil, *Canadian Geotechnical Journal*, **33**, 42–57.